ELSEVIER

0263-8223(95)00089-5

Composite Structures **32** (1995) 313–323

0263-8223/95/$9.50

Filament-wound pressure vessel with thick metal liner

J. M. Lifshitz

Material Mechanics Laboratory, Faculty of Mechanical Engineering, Technion, Israel Institute of Technology, 32000, Haifa, Israel

&

H. Dayan

TAAS-Israel Industries Ltd, Israel

A method for calculating stress and strain in non-symmetric filament-wound pressure vessels with thick metal liners, up to burst pressure, is presented. The calculations are based on classical laminate theory and Tsai-Wu failure criterion. Plastic yielding of the liner and transverse cracking of the composite are not considered failures of the vessel and are modelled by reduced properties. The effect of changing thicknesses of various layers, on burst pressure and efficiency of the vessel, is considered. It is shown that the efficiency of a thick liner reinforced with filament winding can approach optimal values that are quoted in the literature, even when the liner is selected arbitrarily. The calculations agree with test results of two 6 litre vessels having the same liner: one with Kevlar 49/Epoxy overwrap and the other with T300 Carbon/Epoxy.

INTRODUCTION

One area in which the advantages of composite materials, such as high stiffness and strength, can be utilized is that of pressure vessels. The state-of-the-art of the application of composites in pressure vessels and piping until 1977 was reviewed in the Energy Technology conference in Houston, Texas in 1977.[1] This included vessels with various types of liners: elastomers, that carry no load, and metals that may carry part of the load, depending on liner's thickness. In later years a number of studies were conducted on the optimization of filament wound pressure vessels,[2–9] most of them dealing with symmetrically laminated walls without a liner and having a single helical angle of winding. In such a construction, first ply failure is considered total failure of the vessel. When the vessel is constructed by filament winding over a metal liner, in more than one direction, the wall is no longer symmetric and first ply failure does not necessarily mean total failure of the vessel. Failure modes of filament wound aluminium cylinders are considered in Ref. 10 and some applications of filament-wound aluminium liners are described in Refs 11–12. There are basically two approaches to the implementation of composite materials in high pressure vessels:[13] (a) to reinforce a thin metal liner with composite overwrap and (b) to use a thick metal liner reinforced with composite overwrap. The choice of metal for the liners is required whenever the vessel is designed to contain gas under high pressure, in order to prevent diffusion through the wall, or when it is designed to contain liquid under severe temperature conditions. In both cases elastomeric liners are not suitable. Thin liners are not considered to contribute to the load carrying capacity of the vessel, in contrast to thick liners that may support from one-third to one-half of the internal pressure load of the vessel.

Metal liners are normally made of elasto-plastic materials with a large plastic range such as 6061-T6 aluminium. The fibers of the composite material can be carbon, glass or kevlar. One of the advantages of combining a load-bearing

metal liner with composite overwrap is achieved by introducing internal stresses (compression in the liner and tension in the fibers) before putting the vessel to service. This process which is known as 'autofrettage' in metal working, is termed 'sizing' in the composite pressure vessel industry.[14] After fabrication, a sizing pressure, higher than the operating pressure, is applied such that the metal liner is plastically deformed whereas the composite reinforcement is in its elastic range. The elastic unloading of the vessel leaves the liner in compression and the composite reinforcement in tension. Later, in subsequent loading cycles, the entire pressure vessel operates in the enhanced elastic range. The weight saving that can be reached, with load-bearing metal liner reinforced with composite overwrap, compared to all metal vessel, is about 50%.

Thin liners provide higher load-to-weight ratio than thick liners, but they have other problems, like buckling during the decompression phase and difficulties in manufacturing. Thick liners (of a few mm) are more readily available and can be used for manufacturing a composite pressure vessel, which is superior to all metal design, even when the liner itself is not of optimized dimensions.

Safety considerations require that pressure vessels be tested under severe conditions before being approved for commercial use. An essential requirement is to test the vessel up to burst pressure, which is much higher than operating pressure. In the process of this test a few secondary failures, such as plastic yielding of the liner or transverse cracking of the composite layers, take place. Our objective is to calculate the burst pressure of a pressure vessel made of a thick 6061-T6 aluminium liner overwrapped with Kevlar 49 or with T300 Carbon/Epoxy, based on a model of reduced properties, and to compare the predicted values to test results. In doing so, the effect of changing the thickness and orientation of the layers on the burst pressure are also investigated.

The wall of the vessel is made of non-symmetric layup of two different materials. This requires special consideration when the stresses and strains are calculated using the classical laminate theory, particularly after each local failure. Details and justification of the method of calculation are presented in the next section.

A six litre cylindrical pressure vessel, with Kevlar/Epoxy overwrap, was designed, fabricated and tested. The test results compared well with prediction. Although the liner was not optimized, the composite vessel was 45% lighter than an all-metal vessel and still had a higher safety factor than required. To check the validity of the method of calculation for a different composite overwrap, a second vessel, made of the same liner but with T300 Carbon/Epoxy overwrap was designed, fabricated and tested. The results of the second vessel were also in agreement with the prediction.

DESIGN OF THE COMPOSITE VESSEL

(a) General

The problem was to design a six litre cylindrical pressure vessel bounded by given outside dimensions and weight, that would contain oxygen at 150 atmospheres and meet DOT FRP-1 and DOT-E 8162 specifications. The concept that was chosen was of a thick aluminium liner, composed of a long cylindrical section bounded by two caps, and Kevlar 49 fibers in an epoxy resin. Since liners were not readily available, a seamless 6061-T6 aluminium liner that seemed to be suitable was selected from the limited choice that was available, without trying to optimize its dimensions. Some details of the liner are:

outside diameter:	$D_0 = 139$ mm
wall thickness:	$t = 4{\cdot}5$ mm
total length:	$L = 520$ mm
outside dia. of opening:	$d_0 = 43{\cdot}6$ mm
mass:	$M_1 = 3{\cdot}25$ Kg

Some of the important design requirements of the complete vessel are listed below,

outside diameter:	$D < 146{\cdot}5$ mm
total mass:	$M < 4{\cdot}75$ Kg
operating pressure:	$P_0 = 14{\cdot}7$ MPa (150 atm)
proof pressure:	$P_p = 24{\cdot}5$ MPa (250 atm)
burst pressure:	$P_b = 44{\cdot}1$ MPa (450 atm)

The stress analysis presented here deals with the cylindrical section, where the failure is expected to take place, away from the end sections.

The reinforcement consists of helical and hoop winding, with the helical angle α (between the fiber direction and the longitudinal axis of the vessel) determined from the relation given

by Dharmarajan,[15]

$$\sin \alpha = d_0/D_0 \tag{1}$$

The result is: $\alpha = 18{\cdot}3°$.

(b) Stress–strain calculation

In his book *Composite design*, Tsai[16] developed the stress analysis of thick cylindrical vessels as a three dimensional elasticity problem. He compared burst pressure calculations from thin wall and thick wall solutions and concluded that for wall thickness ratios (outside radius/inside radius) $\leq 1{\cdot}10$ the thin wall approximation is adequate.

Calculation of stress and strain in thin walled pressure vessels, away from the closure sections, is done by first calculating the average tensile loads (per unit length) in the axial (N_x) and hoop (N_y) directions and then by the use of load deformation relation of composite laminates. This is fairly simple and raises no questions when the cylindrical wall is made of a symmetric lay up. In such cases the coupling stiffness matrix [**B**] is zero and there is no coupling between extension and bending of the laminate. When the wall is made of a non-symmetric lay up, as in our case, the coupling stiffness does not vanish. Application of bi-axial tensile load to such a laminate would result in both extension and change of curvature of the laminate. This is obviously not possible in the present case, due to the axisymmetric nature of the structure and the load.

In a filament winding process, adjacent layers with $+\alpha$ and $-\alpha$ fiber direction are interleaved and can be considered as a single orthotropic unit.[16] In calculating the reduced stiffness matrix of such a unit, the elements of the reduced stiffness matrix, of a unidirectional layer, that are even functions of the fiber orientation (α) remain unchanged, while the elements that are odd functions of the fiber orientation cancel each other. Thus the interleaved configuration is a specially orthotropic layer with a reduced stiffness matrix:

$$[\mathbf{Q}^{(\alpha)}] = \begin{bmatrix} Q_{xx} & Q_{xy} & 0 \\ Q_{xy} & Q_{yy} & 0 \\ 0 & 0 & Q_{ss} \end{bmatrix} \tag{2}$$

The individual components of the $\mathbf{Q}^{(\alpha)}$ matrix are calculated by the usual transformation relations between the principal material axes and the laminate axes. The other layers of the cylindrical wall are either specially orthotropic (90°) or isotropic (liner), so that the stiffness matrices of the laminate that constitutes the wall are of the following form,

$$[\mathbf{A}] = \begin{bmatrix} A_{xx} & A_{xy} & 0 \\ A_{xy} & A_{yy} & 0 \\ 0 & 0 & A_{ss} \end{bmatrix}$$

$$[\mathbf{B}] = \begin{bmatrix} B_{xx} & B_{xy} & 0 \\ B_{xy} & B_{yy} & 0 \\ 0 & 0 & B_{ss} \end{bmatrix} \tag{3}$$

$$[\mathbf{D}] = \begin{bmatrix} D_{xx} & D_{xy} & 0 \\ D_{xy} & D_{yy} & 0 \\ 0 & 0 & D_{ss} \end{bmatrix}$$

Symmetry considerations prevent the cylindrical wall from undergoing any change of curvature ($\{\kappa\} = 0$). Thus, the general load deformation relation

$$\begin{Bmatrix} N \\ M \end{Bmatrix} = \begin{bmatrix} A & B \\ B & D \end{bmatrix} \begin{Bmatrix} \varepsilon \\ \kappa \end{Bmatrix} \tag{4}$$

is reduced to two uncoupled relations

$$\begin{Bmatrix} N_x \\ N_y \\ 0 \end{Bmatrix} = \begin{bmatrix} A_{xx} & A_{xy} & 0 \\ A_{xy} & A_{yy} & 0 \\ 0 & 0 & A_{ss} \end{bmatrix} \begin{Bmatrix} \varepsilon_x \\ \varepsilon_y \\ \gamma_{xy} \end{Bmatrix} \tag{5}$$

$$\begin{Bmatrix} M_x \\ M_y \\ M_{xy} \end{Bmatrix} = \begin{bmatrix} B_{xx} & B_{xy} & 0 \\ B_{xy} & B_{yy} & 0 \\ 0 & 0 & B_{ss} \end{bmatrix} \begin{Bmatrix} \varepsilon_x \\ \varepsilon_y \\ \gamma_{xy} \end{Bmatrix} \tag{6}$$

From eqn (5) it is clear that the in-plane shear γ_{xy} vanishes and when this is substituted in eqn (6), the twisting moment M_{xy} also vanishes. The load deflection relations for an element of the wall is then

$$\begin{Bmatrix} N_x \\ N_y \\ 0 \end{Bmatrix} = \begin{bmatrix} A_{xx} & A_{xy} & 0 \\ A_{xy} & A_{yy} & 0 \\ 0 & 0 & A_{ss} \end{bmatrix} \begin{Bmatrix} \varepsilon_x \\ \varepsilon_y \\ 0 \end{Bmatrix} ;$$

$$\begin{Bmatrix} M_x \\ M_y \\ 0 \end{Bmatrix} = \begin{bmatrix} B_{xx} & B_{xy} & 0 \\ B_{xy} & B_{yy} & 0 \\ 0 & 0 & B_{ss} \end{bmatrix} \begin{Bmatrix} \varepsilon_x \\ \varepsilon_y \\ 0 \end{Bmatrix} \tag{7}$$

We see that in order to keep the curvature of the non-symmetric wall unchanged by the internal pressure, a self equilibrating internal bending moment $\{M\}$ must be developed in addition to the bi-axial tensile load $\{N\}$. This moment is not known *a priori* and therefore cannot be given explicitly as part of the applied load. Most simple codes that calculate stress and strain in laminates deal with situations where the load is prescribed over the boundaries of the laminated element. They do not cover situations of mixed boundary conditions, as in our case, where partial loads $\{N\}$ and deformations $\{\kappa\}$ are prescribed.

If we try to calculate the strains $\{\varepsilon\}$, in the non-symmetric wall, using such a simple code and assuming that there is no bending moment, we'll get an incorrect result that includes also changes of curvature. Finally, it is important to state that the bending moments do not enter into the calculation of the strains, which are derived from eqn (5).

An alternative way of calculating strains in the non-symmetric thin wall is to assume that the wall thickness is doubled, by adding to the wall its mirror image. The coupling stiffness matrix [**B**] of the new symmetric wall vanishes and the strains are also calculated from eqn (5). The only difference between eqn (5) of the symmetric and non-symmetric laminates is in the values of the matrices [**A**]: the one corresponding to the symmetric laminate is twice the one of the non-symmetric wall. This means that the internal pressure that causes failure in the original non-symmetric wall is half the pressure needed to fail the thicker, symmetric wall. The strains $\{\varepsilon\}$ at failure are the same in the two walls and there is no change of curvature in both cases. The stress distribution through the thickness in the symmetric wall does not give rise to any moments, whereas in the non-symmetric case bending moments are developed in the wall, as shown by eqn (7).

(c) Initial condition of the vessel

The composite overwrap is cured at a relatively low temperature of 60°C. The thermal expansion of the liner squeezes out the excess amount of resin before hardening of the matrix, such that the liner remains almost stress free. Upon cooling to room temperature, residual thermal stresses are developed in the composite layers and a small gap is opened between the liner, which is normally coated with a release agent, and the composite. When the vessel is loaded for the first time, all the load is taken by the liner until the gap is closed. Only then is the additional load distributed between the liner and the overwrap.

To calculate the radial gap Δu, the coefficients of thermal expansion of the composite overwrap $\{\bar{\alpha}\}_{x,y}$ must be calculated first, as shown in Ref. 17,

$$\begin{Bmatrix} \bar{\alpha}_x \\ \bar{\alpha}_y \\ \bar{\alpha}_{xy} \end{Bmatrix} = [\mathbf{A}_c]^{-1} \begin{Bmatrix} N_x^T \\ N_y^T \\ N_{xy}^T \end{Bmatrix} \tag{8}$$

where $[\mathbf{A}_c]^{-1}$ is the inverse of the composite overwrap stiffness matrix and the thermal forces $\{N^T\}$ are given by,

$$\begin{Bmatrix} N_x^T \\ N_y^T \\ N_{xy}^T \end{Bmatrix} = \sum_{k=2}^{n} \begin{bmatrix} Q_{xx} & Q_{xy} & 0 \\ Q_{xy} & Q_{yy} & 0 \\ 0 & 0 & Q_{ss} \end{bmatrix}_k \begin{Bmatrix} \alpha_x \\ \alpha_y \\ \alpha_{xy} \end{Bmatrix}_k t_k \tag{9}$$

Note that the summation is carried only on the layers of the composite overwrap. t_k is the thickness of layer k and $\{\alpha\}_{x,y;k}$ are the coefficients of thermal expansion of layer k, in the vessel's (x, y) coordinates.

Now the radial gap can be calculated,

$$\Delta u = (\bar{\alpha}_y R_c - \alpha_l R_l)\Delta T \tag{10}$$

where R_c and R_l are the average radii of the composite and liner respectively; ΔT is the temperature drop (negative) from the curing to room temperature, and α_l is the coefficient of thermal expansion of the liner.

The internal pressure required to close this gap is

$$p_a = \frac{2E_l \Delta u t_l}{R_l^2(2 - \nu_l)} \tag{11}$$

E and ν are Young's modulus and Poisson's ratio and the subscript l indicates 'liner'.

The residual thermal stresses in layer k are calculated after subtracting from the laminate thermal strain the thermal strain of the free lamina k,

$$\begin{Bmatrix} \varepsilon_1^T \\ \varepsilon_2^T \\ \gamma_{12}^T \end{Bmatrix}_k = [\mathbf{R}] \left\{ [\mathbf{T}] \begin{Bmatrix} \bar{\alpha}_x \\ \bar{\alpha}_y \\ \frac{1}{2}\bar{\alpha}_{xy} \end{Bmatrix} - \begin{Bmatrix} \alpha_1 \\ \alpha_2 \\ 0 \end{Bmatrix}_k \right\} \Delta T \quad (12)$$

$$\begin{Bmatrix} \sigma_1^T \\ \sigma_2^T \\ \sigma_{12}^T \end{Bmatrix}_k = \begin{bmatrix} Q_{11} & Q_{12} & 0 \\ Q_{12} & Q_{22} & 0 \\ 0 & 0 & Q_{66} \end{bmatrix}_k \begin{Bmatrix} \varepsilon_1^T \\ \varepsilon_2^T \\ \gamma_{12}^T \end{Bmatrix} \quad (13)$$

where

$$[\mathbf{R}] = \begin{bmatrix} 1 & 0 & 0 \\ 0 & 1 & 0 \\ 0 & 0 & 2 \end{bmatrix}$$

is due to Reuter,[18] and

$$[\mathbf{T}] = \begin{bmatrix} m^2 & n^2 & 2mn \\ n^2 & m^2 & -2mn \\ -mn & mn & m^2-n^2 \end{bmatrix}; \quad \begin{matrix} m=\cos\theta \\ n=\sin\theta \end{matrix}$$

is the transformation matrix.

The closing of the gap can be seen in Fig. 1 which gives the relation between internal pressure and hoop strain, measured on the external surface of the Kevlar/Epoxy overwrap. It shows that up to a pressure of about 5 MPa, (point '*a*' in the figure), the gap is not yet closed and the composite overwrap is not loaded by the internal pressure. This phenomenon is characteristic of vessels that are loaded for the first time. The other points, indicated on the graph by *b*, *c*, *d*, are points of local failure as explained in the next section.

(d) Stress–strain calculation after first ply failure

Three types of failure are considered: (a) plastic yielding of the liner; (b) transverse cracking of composite layers; (c) fiber breaking. Only the last is considered as failure of the pressure vessel. The other two lead to reduction of some properties as given in Table 1.

The method of calculating the pressure vs. hoop strain up to burst pressure is demonstrated for a vessel made by overwraping the aluminium liner with two helical units (each 0·4 mm thick) and 1·8 mm thick hoop winding (nine layers, each 0·2 mm thick), made of Kevlar 49/Epoxy. The moduli and strength values used in the calculations are listed in Table 1, where the subscripts '*t*' and '*c*' indicate tension and compression.

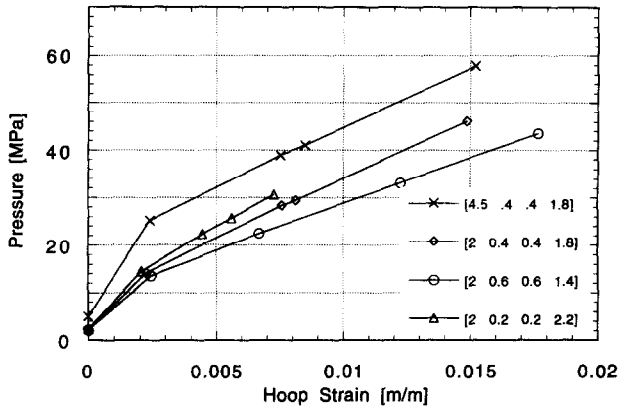

Fig. 1. Pressure vs. hoop strain in a Kevlar/Epoxy reinforced pressure vessel.

Failure of the layers is determined by the Tsai-Wu failure criterion, which is reduced to the von Mises yield criterion for the isotropic liner. The first layer to fail is the liner, that yields plastically when the internal pressure reaches 25·1 MPa (point '*b*' in Fig. 1). The stresses and strains in each layer, corresponding to point '*b*', are calculated and used as initial conditions for the next loading step. Now the loading continues and the additional stresses and strains are calculated based on the reduced properties of the wall, that are obtained by replacing the properties of the virgin aluminium (column 2 in the table) by the values in column 3.

The next failure (point '*c*') is transverse cracking of the $\pm 18{\cdot}3°$ layers at 38·9 MPa. The new reduced stiffness of the wall is calculated by replacing the properties of the helical layers with the values from column 7 in the table. The initial condition for calculating the next failure is again point '*b*', but with the current reduced properties. The calculations show that the next failure is transverse cracking of the hoop layers (point '*d*') at 41 MPa. For simplicity, the failure points are connected by straight lines. This process is repeated once again, now with all the layers having reduced properties. The failure under these conditions is catastrophic, due to fiber breaking (point '*e*') in the helical layers at

Table 1. Properties of constituent materials

Property	Al 6061-T6		T300/Epoxy		Kevlar/Epoxy	
	Virgin	Plastic	Virgin	Cracked	Virgin	Cracked
E_{11} (GPa)	69·5	0·1	123	123	86·3	86·3
E_{22} (GPa)	69·5	0·1	8·3	0·08	4·9	0·05
G_{12} (GPa)	26·7	0·1	4·3	0·04	2	0·02
ν_{12}	0·3	0·5	0·27	0·27	0·34	0·34
F_{1t} (MPa)	240	278	1275	1275	1520	1520
F_{1c} (MPa)	240	278	1275	1275	333	333
F_{2t} (MPa)	240	278	49	0	29	0
F_{2c} (MPa)	240	278	216	0	157	0
F_6 (MPa)	137	137	69	0	49	0

57·8 MPa (589 atm). The experimental burst pressure was 600 atm. It is interesting to observe that the pressure vs. hoop strain is close to a response of a bi-linear material with a yield point that coincides with the yielding of the liner.

RESULTS AND DISCUSSION

(a) Changing the angle of the helical layers

Although the helical angle is determined by eqn (1), it is possible to increase or decrease it by some degrees. Figure 2 shows that the effect of such changes on the performance of the vessel is not very large. An increase of the helical angle leads to a decrease in the burst pressure and strain. However, technical limitations on the helical angle rule out small winding angles. The conclusion from the figure is that there is no justification to deviate from the recommended angle given by eqn (1).

A measure of the efficiency of the overwrap winding can be the ratio (at burst) between the stress σ_1 in the fiber direction, in the layers without fiber failure, and the longitudinal tensile strength F_{1t}. These ratios, corresponding to the results presented in Fig. 2, are (from 15° to 27°): 0·905, 0·865, 0·809, 0·724. Thus, at burst pressure, the stress in the fiber direction in the hoop layers, of the 15° helical vessel, reaches 0·905 of its ultimate strength. On the other end, for the 27° helical vessel, the stress in the hoop layers is only 0·724 of the ultimate strength and therefore they do not contribute their proper share in carrying the load.

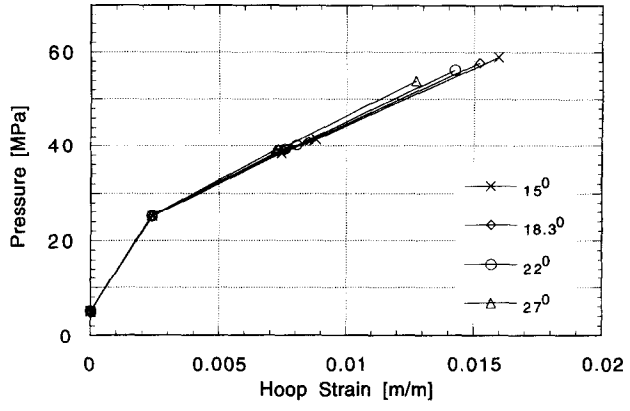

Fig. 2. Pressure vs. hoop strain for a Kevlar/Epoxy reinforced pressure vessel for various angles of overwrap.

(b) Changing the ratio between the number of hoop and helical layers

The present design has two helical units ($\pm 18{\cdot}3°$), each of thickness 0·4 mm, and nine hoop layers (90°), each of thickness 0·2 mm. Two variations, of the same total thickness are considered: one with a single helical unit, containing a layer 0·2 mm thick in the $+18{\cdot}3°$ and a layer 0·2 mm thick in the $-18{\cdot}3°$, and eleven hoop layers; the other with three helical units and seven hoop layers. The results are shown in Fig. 3, where the thickness of the various layers are typed in the figure, in square brackets, in the following order: [liner $+\alpha^0-\alpha^0$ hoop]. The highest burst pressure (57·8 MPa) is obtained for the present design [4·5 0·4 0·4 1·8]. The lowest burst pressure (42·6 MPa) is obtained for the vessel with the eleven hoop layers [4·5 0·2 0·2 2·2] and the intermediate pressure (54·3 MPa) is for the vessel with seven hoop layers [4·5 0·6 0·6 1·4]. When the stress in the

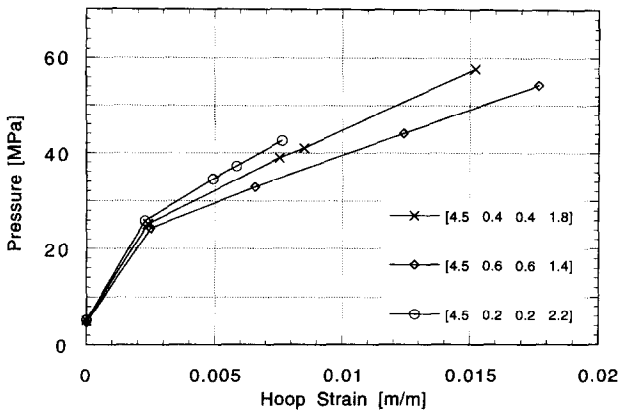

Fig. 3. Effect of hoop-to-helical thickness ratio on the burst pressure of a Kevlar/Epoxy vessel with 4·5 mm thick liner.

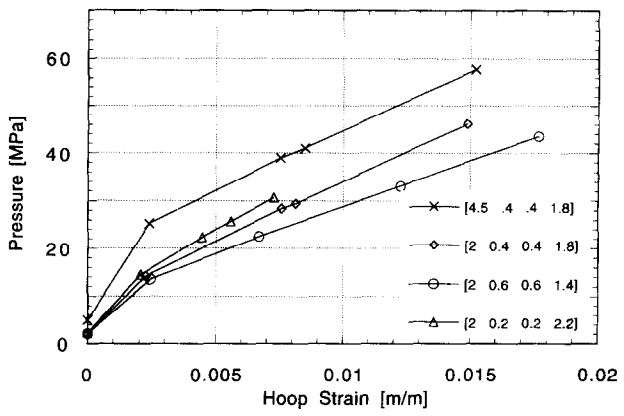

Fig. 4. Effect of hoop-to-helical thickness ratio on the burst pressure of a Kevlar/Epoxy vessel with 2 mm thick liner.

fiber direction, in the layers without fiber failure, is normalized with respect to the longitudinal strength F_{1t}, the ratio for the present design is 0·865. This indicates that when the fibers fail in the helical layers, the hoop layers reach almost their full potential as load carrying. The ratio for the design where four hoop layers are transformed to a pair of helical layers [4·5 0·6 0·6 1·4] is 0·634, which indicates that the burst pressure is also lower. The calculations predict that by this transfer of hoop to helical layers, the location of catastrophic failure (fiber fracture) moves from the helical layers to the hoop layers. The result is an increase in the fracture hoop strain, to the ultimate longitudinal tensile strain. The last curve in Fig. 3 is for a wall where a pair of helical layers are transformed to hoop layers [4·5 0·2 0·2 2·2] and the appropriate stress ratio is 0·432. This indeed is a very low value which agrees with the predicted low value of burst pressure. The location of fiber failure in this design is back in the helical layers.

A similarly check, of changing the ratio between the number of hoop and helical layers, was done for a vessel with a 2 mm thick liner, with similar conclusions. The results are shown in Fig. 4, which includes the curve of the present 4·5 mm liner design as a reference. The lower burst pressure of the three variations is expected due to the reduction in load carrying capacity of the thinner liner. The other features are quite similar to those of Fig. 3 and among the three possibilities of having one, two or three helical units, two is the preferred choice. The normalized stress (σ_1/F_{1t}) in the fiber direction in layers without fiber failure is 0·845 for the [2 0·4 0·4 1·8] configuration; 0·644 for the [2 0·6 0·6 1·4] configuration; and 0·415 for the [2 0·2 0·2 2·2] one.

The minimum layer thickness of the composite used in this study is 0·2 mm. This constrains the ratio between helical to hoop thickness to discrete values and prevents the possibility of designing for simultaneous fiber failure in all the layers. Theoretically, as the layers get thinner, the burst pressure can reach a maximum value.

(c) Changing the thickness ratio between liner and composite

The performance of the vessel can be dramatically improved, keeping the total weight unchanged, by reducing the thickness of the liner and increasing the thickness of the composite overwrap (Fig. 5). By reducing the liner thickness to 2 mm, the composite thickness of the Kevlar 49/Epoxy can be increased to 7·6 mm. To keep the ratio between the hoop and the helical layers close to the original design, we need to have six helical units and twenty six hoop layers [2 1·2 1·2 5·2]. The burst pressure for such a vessel is calculated to be 117·5 MPa, with fiber failure in the helical layers. Reducing the number of hoop layers to twenty four and transfering the reinforcement to the helical layers [2 1·4 1·4 4·8] increases the burst pressure to 127·8 MPa, with fiber failure in the hoop layers at 1·76% hoop strain. Additional transfer of hoop to helical layers namely [2 1·6 1·6 4·4] is of no use and decreases the burst pressure to (118·2 MPa), leaving the location of fiber failure in the hoop layers. If the change of the

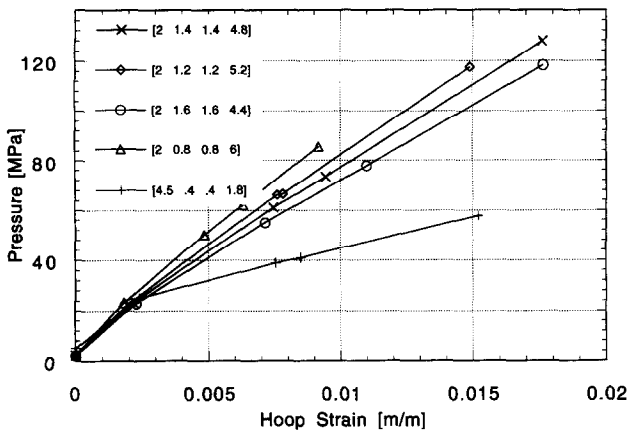

Fig. 5. Effect of changing thickness between liner and overwrap in a constant weight Kevlar/Epoxy vessel.

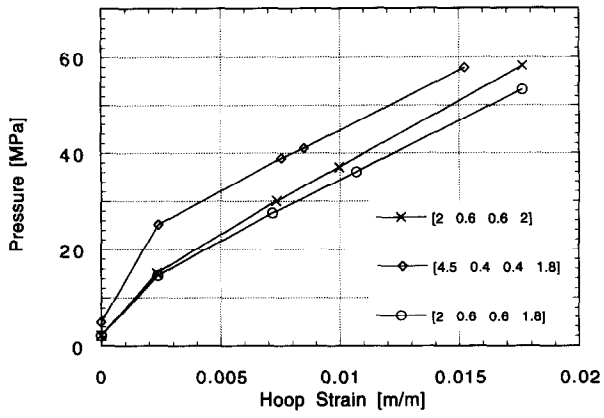

Fig. 6. Comparing Kevlar/Epoxy reinforced 2 and 4·5 mm liners for a given burst pressure.

thicknesses is reversed and the number of hoop layers is increased to thirty [2 0·8 0·8 6], the performance is decreased dramatically to a burst pressure of 85·5 MPa, with fiber failure back in the helical layers. These results show the same trend as in Figs 3 and 4 namely, that there is an optimal ratio between the number of hoop and helical layers.

The results in the last paragraph show that the burst pressure of the present 4·5 mm liner design can be more than doubled by transferring weight from the liner to the composite overwrap. Alternatively, the requirement for a burst pressure of about 600 atm (58·8 MPa) can be met with a lighter vessel of 2 mm thick liner, by adding a single hoop layer and one helical unit [2 0·6 0·6 2] to the original overwrap. The result is shown in Fig. 6 together with the present 4·5 mm liner design. The burst pressure of the 2 mm liner design is 58·2 MPa, which is practically the same as the burst pressure of the present 4·5 mm liner design. Removal of a single hoop layer, from the light vessel reduces its burst pressure to 53·3 MPa and removal of a single helical unit (see Fig. 4) reduces the burst pressure to 46·2 MPa.

(d) Efficiency of the pressure vessel

A common way to define efficiency (e) of pressure vessels is by the relation,

$$e = P_b V/W \tag{14}$$

where P_b is the burst pressure, V the volume of the vessel and W the vessel's weight. The mass of the present 4·5 mm thick liner is 3·25 kg and that of the reinforcement 1·01 kg, bringing the total mass to 4·26 kg. The volume is $6{\cdot}038 \times 10^{-3}$ m^3 and the burst pressure is 57·8 MPa. The efficiency, denoted by e_0, is therefore $e_0 = 8{\cdot}354$ m.

This efficiency is considerably lower than the efficiency range of similar vessels (13·970 to 17·780 m) given by Morris *et al.*[19] and can be even lower by selecting wrong combinations of hoop and helical layers. This is to be expected, since the liner is thicker than necessary for optimal design. A much better efficiency can be achieved by reducing the thickness of the liner, as shown in Table 2. Column four shows the sequence of local failures up to fiber fracture. '1' indicates the liner, '2' indicates the helical layers ($+\alpha$ or $-\alpha$) and '4' stands for the hoop layers. Column five gives the ratio, at burst pressure, between the stress in the fiber direction in the layers without fiber fracture, and the corresponding strength F_{1t}.

The results in the table indicate that the reduction of the liner's thickness to 2 mm, followed by some increase in the original composite thickness, improves the efficiency, within the boundaries of the design requirements.

(e) Changing the fibers

To check the methodology presented here, the calculations were repeated for similar vessels, having the same liners (4·5 and 2 mm thick) but overwrap made of T300 Carbon/Epoxy. The helical angle was 20°, to fit the geometry of the vessel that was manufactured. Similar graphs to Figs 1–6 that were drawn for the T300 Carbon/Epoxy vessel, lead to similar conclusions

Table 2. Efficiency of some Kevlar/Epoxy reinforced vessels

Wall structure (mm)	P_b (MPa)	ε_{hoop} (%)	Failure sequence	σ_1/F_{1t}	M_{liner} (kg)	M_{comp} (kg)	e/e_0
[4·5 0·4 0·4 1·8]	57·8	1·52	1→2→4→2	0·865	3·25	1·01	1
[4·5 0·6 0·6 1·4]	54·3	1·76	1→2→4→4	0·634	3·25	1·01	0·94
[4·5 0·2 0·2 2·2]	42·6	0·76	1→4→2→2	0·435	3·25	1·01	0·74
[2 0·4 0·4 1·8]	46·2	1·49	1→2→4→2	0·845	1·44*	1·01	1·39
[2 0·6 0·6 2]	58·2	1·76	1→2→4→4	0·908	1·44	1·24	1·60
[2 1·4 1·4 4·8]	127·8	1·76	1→2→4→4	0·952	1·44	2·95	2·15
[2 1·6 1·6 4·4]	118·2	1·76	1→2→4→4	0·770	1·44	2·95	1·98
[2 1·2 1·2 5·2]	117·5	1·49	1→2→4→2	0·846	1·44	2·95	1·97

*Calculated value.

obtained for the Kevlar/Epoxy vessel. Some of the results are presented in the next three figures.

The structure of the vessel that was built and tested is [4·5 0·8 0·8 3·8]. In Fig. 7, which is similar to Fig. 3, the calculated results for that vessel are compared to other vessels, having the same overwrap total thickness but different ratios between helical and hoop layers. The calculated burst pressure of the real vessel is 84·6 MPa (863 atm) compared to the test value of 860 atm. However, the calculations show that by transferring two hoop layers to a single unit of helical wrap [4·5 1 1 3·4] the burst pressure can be raised to 90·8 MPa. In this process the location of fiber fracture is moved from the helical to the hoop layers and the ratio σ_1/F_{1t} is increased from 0·823 to 0·915.

Next, the effect of keeping the weight of the vessel constant by reducing the thickness of the liner to 2 mm and increasing the overwrap to 9·4 mm is shown in Fig. 8, which is similar to Fig. 5. The best configuration is [2 1·8 1·8 5·8], with burst pressure of 131·2 MPa and stress ratio σ_1/F_{1t} of 0·915. This is a large improvement over the vessel that was built, even though it is less than for the Kevlar/Epoxy vessel.

Figure 9, which is the equivalent of Fig. 6, shows that by adding a single unit of helical layers to the original design and reducing the liner thickness to 2 mm, the burst pressure remains unchanged. Addition of a second helical unit [2 1·2 1·2 3·8] increases the burst pressure even more, to 88·9 (906 atm), with stress ratio σ_1/F_{1t} of 0·953.

Finally, the experimental curve of the T300 Carbon/Epoxy vessel is compared to the calculated values of the local failures in Fig. 10. The agreement is good and the character of the pressure-hoop strain is preserved in the calculations.

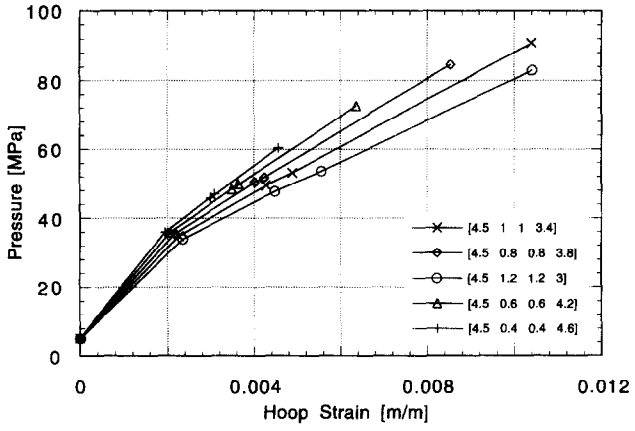

Fig. 7. Effect of hoop-to-helical thickness ratio on the burst pressure of a T300 Carbon/Epoxy vessel with 4·5 mm thick liner.

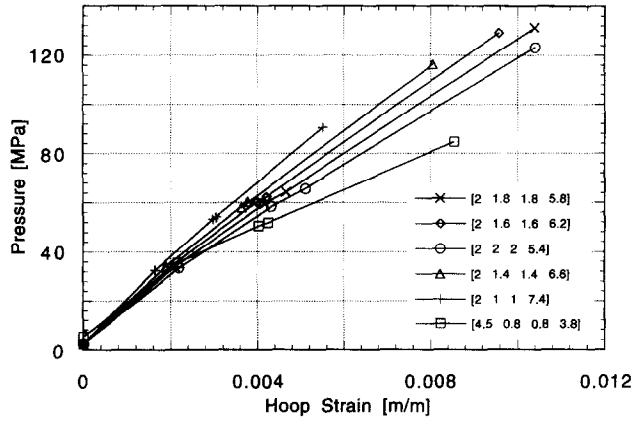

Fig. 8. Effect of changing thickness between liner and overwrap in a constant weight T300 Carbon/Epoxy vessel.

CONCLUSIONS

(1) Stress and strain in a pressure vessel of non-symmetric lamination can be calculated without coupling between the force and moment resultants.

(2) Filament-wound pressure vessel with thick metal liner is superior to all-metal

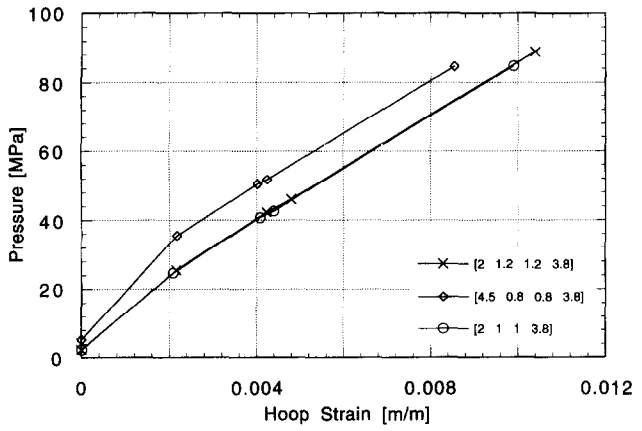

Fig. 9. Comparing T300 Carbon/Epoxy reinforced 2 and 4·5 mm liners for a given burst pressure.

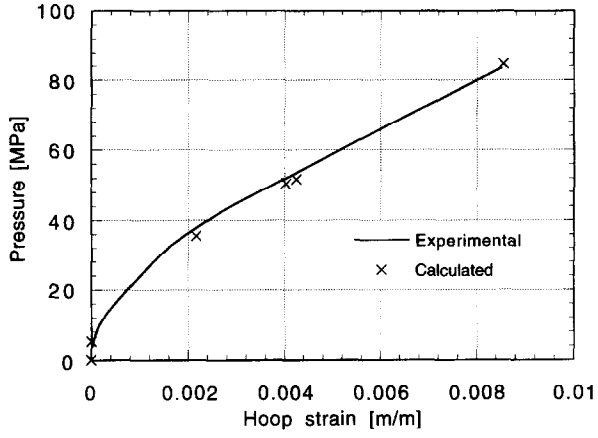

Fig. 10. Experimental and predicted pressure vs. hoop strain in a T300 Carbon/Epoxy reinforced vessel.

vessel, even when the liner is not of optimal thickness.

(3) The efficiency of the vessel can be improved by changing the ratio between hoop and helical layers. The ratio of the stress in the fiber direction (at burst), in the unbroken layer, to the longitudinal composite strength is an indicator of the efficiency. To get optimal design this ratio must approach unity.

(4) Weight transfer from the liner to the overwrap increases the burst pressure and the efficiency. The magnitude of the improvement depends on the moduli and strength of the constituent materials.

(5) *In situ* measurements of mechanical properties of filament-wound vessels are needed in order to determine moduli and strength values, which are not the same as those obtained from unidirectional laminae.

ACKNOWLEDGEMENT

The authors acknowledge the contribution of TAAS-Israel Industries Ltd. in designing, manufacturing and testing the vessels.

REFERENCES

1. Kulkarni, S. V. & Zweben, C. H. (eds), *Composites in Pressire Vessels and Piping*, PVP-PB-021, ASME, 1977.
2. Tauchert, T. R., Optimum design of a reinforced cylindrical pressure vessel. *J. Comp. Mat.*, **15** (1981) 390–402.
3. Fukunaga, H. & Uemura, M., Optimum design of helically wound composite pressure vessels. *J. Comp. Struct.*, **1** (1983) 31–49.
4. Eckold, G. C., A design method for filament wound GRP vessels and pipework. *Comp.*, **16** (1985) 41–47.
5. Fukunaga, H. & Chou, T. W., Simplified design techniques for laminated cylindrical pressure vessels under stiffness and strength constraints. *J. Comp. Mat.*, **22** (1988) 1157–69.
6. Karandikar, H., Srivinvasan, R., Mistree, F. & Fuchs, W. J., Compromise: an effective approach for the design of pressure vessels using composite materials. *Computers & Struct.*, **33** (1989) 1465–77.
7. Adali, S. & Yakar, B., Optimal design of laminated pressure vessels under internal pressure and temperature loading. In *Pressure Vessels and Components 1991, Proc. 1991 Pressure Vessels and Piping Conference* (PVP-Vol. 217). ASME, New York, USA, 1991, pp. 57–63.
8. Adali, S., Fuzzy optimization of laminated cylindrical pressure vessels. In *Composite Structures 6, Proc. 6th International Conference on Composite Structures*. Elsevier Applied Science, London, UK, 1991, pp. 249–259.
9. Adali, S., Sumers, E. B. & Verijenko, V. E., Optimization of laminated cylindrical pressure vessels under strength criterion. *Comp. Struct.*, **25** (1993) 305–312.
10. Teply, J. L. & Herbein, W. C., Failure modes for filament wound aluminum natural gas cylinders. In *The Mechanism of Fracture, Proc. Fracture-Mechanism Prog. & Related Papers, Inter. Conf. & Exposition on Fatigue, Corrosion Cracking, Fracture Mechanics and Failure Analysis*, 2–6 December 1985, Salt Lake City, Utah (ed. Goel, V. S.) ASM, 1986, pp. 327–337.
11. Darms, F. J., Space age pressure vessels. In *36th Inter. SAMPE Symposium and Exhibition*, **36** (1991) 818–826.
12. Young, K. S., Advanced composites storage containment for hydrogen. *Int. J. Hydrogen Energy*, **17** (1992) 505–507.
13. Lark, R. F., Recent advances in lightweight, filament-wound composite pressure vessel technology. In *Composites in Pressure Vessels and Piping* (eds Kulkarni, S. V. & Zweben, C. H.) PVP-PB-021, ASME, 1977, pp. 17–49.
14. Morris, E. E., Patterson, W. P., Landes, R. E. & Gordon, R., Composite pressure vessels for aerospace and commercial applications. In *Composites in Pressure Vessels and Piping* (eds Kulkarni, S. V. & Zweben, C. H.) PVP-PB-021, ASME, 1977, pp. 89–128.
15. Dharmarajan, S., Analysis and design of reinforced plastic components. *Reinforced Plastics — Principles &*

Applications, General Dynamics/Astronautics, San Diego, USA (1963).
16. Tsai, S. W., *Composite Design*, Chap. 23. Think Composites. Dayton, OH, 1987.
17. Daniel, I. M. & Ishai, O., Engineering mechanics of composite materials. Chap. 6. Oxford University Press, Inc. Oxford, UK, 1994.
18. Reuter, R. C. Jr., Concise property transformation relations for an anisotropic lamina. *J. Comp. Mat.*, **5** (1971) 270–272.
19. Morris, E. E., Darms, F. J. & Lynn, V., Lower cost, high performance composite fiber/metal tank for spacecraft. *AIAA/ASME/SAE/ASEE 22nd Joint Propulsion Conference*, 16–18 June 1986, Huntsville, AL, 1986.